

Development and microstructure characterization of single and duplex nitriding of UNS S31803 duplex stainless steel

Tschiptschin, A. P.; Varela, L. B.; Pinedo, C. E.; Li, Xiao-Ying; Dong, Hanshan

DOI:

[10.1016/j.surfcoat.2017.08.018](https://doi.org/10.1016/j.surfcoat.2017.08.018)

License:

Creative Commons: Attribution-NonCommercial-NoDerivs (CC BY-NC-ND)

Document Version

Peer reviewed version

Citation for published version (Harvard):

Tschiptschin, AP, Varela, LB, Pinedo, CE, Li, X-Y & Dong, H 2017, 'Development and microstructure characterization of single and duplex nitriding of UNS S31803 duplex stainless steel', *Surface and Coatings Technology*, vol. 327, pp. 83-92. <https://doi.org/10.1016/j.surfcoat.2017.08.018>

[Link to publication on Research at Birmingham portal](#)

General rights

Unless a licence is specified above, all rights (including copyright and moral rights) in this document are retained by the authors and/or the copyright holders. The express permission of the copyright holder must be obtained for any use of this material other than for purposes permitted by law.

- Users may freely distribute the URL that is used to identify this publication.
- Users may download and/or print one copy of the publication from the University of Birmingham research portal for the purpose of private study or non-commercial research.
- User may use extracts from the document in line with the concept of 'fair dealing' under the Copyright, Designs and Patents Act 1988 (?)
- Users may not further distribute the material nor use it for the purposes of commercial gain.

Where a licence is displayed above, please note the terms and conditions of the licence govern your use of this document.

When citing, please reference the published version.

Take down policy

While the University of Birmingham exercises care and attention in making items available there are rare occasions when an item has been uploaded in error or has been deemed to be commercially or otherwise sensitive.

If you believe that this is the case for this document, please contact UBIRA@lists.bham.ac.uk providing details and we will remove access to the work immediately and investigate.

Accepted Manuscript

Development and microstructure characterization of single and duplex nitriding of UNS S31803 duplex stainless steel

A.P. Tschiptschin, L.B. Varela, C.E. Pinedo, X.Y. Li, H. Dong



PII: S0257-8972(17)30780-6
DOI: doi: [10.1016/j.surfcoat.2017.08.018](https://doi.org/10.1016/j.surfcoat.2017.08.018)
Reference: SCT 22579
To appear in: *Surface & Coatings Technology*
Received date: 26 March 2017
Revised date: 25 June 2017
Accepted date: 1 August 2017

Please cite this article as: A.P. Tschiptschin, L.B. Varela, C.E. Pinedo, X.Y. Li, H. Dong , Development and microstructure characterization of single and duplex nitriding of UNS S31803 duplex stainless steel, *Surface & Coatings Technology* (2017), doi: [10.1016/j.surfcoat.2017.08.018](https://doi.org/10.1016/j.surfcoat.2017.08.018)

This is a PDF file of an unedited manuscript that has been accepted for publication. As a service to our customers we are providing this early version of the manuscript. The manuscript will undergo copyediting, typesetting, and review of the resulting proof before it is published in its final form. Please note that during the production process errors may be discovered which could affect the content, and all legal disclaimers that apply to the journal pertain.

Development and Microstructure Characterization of Single and Duplex Nitriding of UNS S31803 Duplex Stainless Steel

A.P. Tschiptschin^{1,#}, L.B. Varela¹, C.E. Pinedo², X.Y. Li³, H. Dong³

¹Department of Metallurgical and Materials Engineering, University of São Paulo, Av. Prof. Mello Moraes 2463, ZIP 05508-030, São Paulo, SP, Brazil.

²Heat Tech Technology for Heat Treatment and Surface Engineering Ltd, Av. João XXIII 1160, ZIP 08830-000, Mogi das Cruzes, SP, Brazil.

³School of Metallurgy and Materials, College of Engineering and Physical Sciences, The University of Birmingham, Birmingham B15 2TT, UK.

Corresponding author's phone: +55-11-30915656 E-mail: antschip@usp.br

Abstract

In this work, the development of a duplex nitriding (DN) surface treatment combining High Temperature Gas Nitriding (HTGN) and Low Temperature Plasma Nitriding (LTPN) is reported. The microstructure and hardness variation of the duplex treated steel is compared with the properties obtained during single HTGN and single LTPN of UNS S31803 stainless steel. Single LTPN of UNS S31803 was carried out in an Active Screen Plasma Nitriding reactor, at 400 °C for 20 h, in a 75 % N₂ + 25 % H₂ atmosphere. Single HTGN of UNS S31803 was carried out at 1200 °C, under a 0.1 MPa high purity N₂ gas atmosphere, during 8 hours. The developed duplex nitriding (DN) surface treatment consists of a combination of both, HTGN and LTPN treatments, carried out in the same conditions described above.

The microstructure of the as received material was composed by ferrite and austenitic stringers, aligned in the rolling direction. The results showed that LTPN of the UNS S31803 duplex stainless steel promotes the formation of a duplex modulated structure composed by 2.5 µm thick, 1510 ± 52 HV hard, expanded ferrite (α_N) regions, and 3.0 µm thick, 1360 ± 81 HV hard, expanded austenite (γ_N) regions on ferrite and austenite grains, respectively. Intense coherent ε-Fe₃N nitride

precipitation inside expanded ferrite was observed. ϵ -Fe₃N nitrides precipitated with an orientation relationship $[111] \alpha_N // [120] \epsilon$ -Fe₃N, leading to increased microhardness of the expanded ferrite regions. After the first step of the duplex nitriding treatment (HTGN) a 550 μm thick, 330 HV hard, nitrogen rich, fully austenitic layer formed at the surface of the specimens, by transformation of ferrite stringers into austenite. The second nitriding step (LTPN) led to the formation of a homogeneous expanded austenite layer, 1227 ± 78 HV on top of the thick fully austenitic layer, formed during the first step. The duplex treatment resulted in a more homogeneous, precipitate-free, microstructure and a better transition between the mechanical properties of the hardened outermost layer and the softer substrate.

Keywords: Duplex stainless steel; High temperature gas nitriding; Low temperature plasma nitriding; Duplex nitriding treatment.

1. Introduction

Duplex stainless steels (DSS) are widely used in high performance components for oil and gas, nuclear, chemical and paper industries, due to its superior combination of strength and corrosion resistance, compared to austenitic stainless steels [1]. However, for some applications, where outstanding wear resistance is required, the bulk hardness is not high enough to guarantee the best performance. In such applications, the use of surface treatments to increase surface hardness is an important technological solution to improve the tribological performance and the components' life performance.

Low Temperature Plasma Nitriding (LTPN) has proved to be a successful option to increase surface hardness and wear resistance, without impairing the corrosion resistance of austenitic, martensitic and ferritic stainless steels [2-4]. Low temperature nitriding, carried out at temperatures lower than 430°C, can avoid nitride precipitation, leading to nitrogen supersaturation and formation of expanded austenite, expanded ferrite or expanded martensite. Such supersaturation results in

expansion of the crystal lattice and creation of very intense compressive residual stresses leading to an increase of the surface hardness due to the formation of these expanded phases. Moreover, at low temperature, chromium nitrides precipitation is avoided. Even if iron nitrides precipitate, chromium depletion does not occur maintaining the corrosion properties of the steel.

LTPN of austenitic stainless steels has been discussed in literature, providing a rather well defined nitriding mechanism, associated with the formation of S-phase or expanded austenite. Nevertheless, published papers dealing with LTPN of duplex stainless steels are scarce in literature, the mechanisms of surface hardening are not quite well understood and some controversy still exists related to the formation of expanded austenite all over the nitrided case. Blawert et al. [5] described a nitrogen promoted phase transformation of pre-existing ferrite into expanded austenite at the surface of LTPN DSS specimens. Bielawski et al. [6] reported the formation of nitrogen-enriched layers, containing an “expanded austenite like” layer obtained on top of the ferritic regions of the matrix. Some years later, the same authors [7] reported the formation of expanded martensite on the ferrite grains of the matrix. Christiansen et al. [8], instead, reported the formation of a thick layer of expanded austenite on both ferrite and austenite grains of the matrix in a SAF 2507 superduplex stainless steel. Chiu et al. [9] reported the formation of expanded ferrite and expanded austenite on ferrite and austenite stringers of an UNS S31803 duplex, respectively.

Nagatsuka et al. [10] discussed the formation of a nitrided case on top of ferrite grains and concluded that S phase (expanded austenite) was uniformly formed on both austenitic and ferritic phases, after ASPN at 450 °C. In a previous work, Pinedo et al. [11] found that the nitrided layer was composed by a modulated structure developed on the surface of the specimen, containing expanded austenite and expanded ferrite, with the expanded ferrite layer being thicker than the neighboring expanded austenite layer. The expanded ferrite phase showed acicular structures crossing the layer, suggesting that deformation bands propagated inside this phase due to intense compressive stresses developed during nitriding [11].

Literature reporting the mechanical and tribological (wear) behaviour of low temperature nitrided duplex stainless steel is scarce. Nagatsuka et al. [10] studied the wear behavior of low temperature active screen plasma nitrided duplex stainless steel and concluded that wear resistance was greater for active screen plasma nitriding than for DC plasma nitriding.

When submitted to high loading conditions, single LTPN duplex stainless steel may prematurely fail as the thin and hard expanded austenite / expanded ferrite layers may collapse, mainly due to substrate elastic and plastic deformations, the so called eggshell-effect [12]. Mesa et al [13], studying the cavitation-erosion behavior duplex stainless steel developed a sequence of nitriding treatments that resulted in a cavitation-erosion resistance 180 times greater than 304 stainless steel and 23 times greater than LTPN 304 stainless steel. The proposed duplex nitriding treatment (HTGN+LTPN) was composed by a high temperature gas nitriding step (HTGN), carried out in a pure nitrogen atmosphere at 1200°C, for 8 hours, at 0.1 MPa pressure, followed by a low temperature plasma nitriding step (LTPN) carried out at 400°C, for 20 h at 400 Pa pressure. The resulting duplex nitrided structure consisted of a thick layer of nitrogen rich austenite, followed by a much thinner expanded austenite layer formed by LTPN. The increased substrate hardness granted mechanical support to the thinner and harder expanded austenite layer, assuring greater adhesion of the hard expanded austenite layer formed on top of the duplex stainless steel, assuring much greater cavitation wear resistance [13].

The aim of this paper is to analyse the microstructural changes involved in single LTPN and duplex (HTGN + LTPN) surface treatments of UNS S31803, in order to better understand the mechanisms of the undergoing phase transformations and better control the nitriding parameters assuring good tribological and micromechanical properties to the thermochemical treated alloy.

2 Experimental

Wrought round bars of solution treated UNS S31803 duplex stainless steel were cut in 5 mm thick slices. The analyzed chemical composition is shown in Table 1.

Table 1. Chemical composition in mass %

C	Cr	Ni	Mo	N	Si	P	S
0.016	22.60	4.30	3.06	0.20	0.66	0.009	0.001

The specimens were fine ground and diamond polished before surface treatments. High Temperature Gas Nitriding (HTGN) was carried out in a horizontal cylindrical chamber furnace at 1200°C in a pure N₂ (99.999% purity) atmosphere, under 0.1 MPa pressure, during 8 hours. Low Temperature Plasma Nitriding treatments (LTPN) were carried out in a Plasma Metal SA-Luxemburg DC-pulsed plasma active plasma screen reactor at 400°C, using a gas mixture of 75% N₂+25% H₂, under 400 Pa pressure and 20 hours, with a bias voltage of 320 V. The carbon steel active screen was 1.5 m in diameter and 1.8 m high. The specimens were arranged in a circle equidistant 30 cm from the screen walls and distant \approx 1.3 m from its top.

The microstructure at the specimens' surface was analyzed by light optical microscopy (LOM) and scanning electron microscopy (SEM). WDS analysis of the nitrogen content at the surface of the HTGN layer was carried out in an Oxford spectrometer coupled to a Cambridge Stereoscan 440 SEM, using a procedure developed by Toro et al. [14].

Wavelength dispersive analysis was carried out in an Oxford WDX600 spectrometer with take-off angle 35°, coupled to a Cambridge Stereoscan 440 SEM equipped with LaB6 emission source operating at 10 kV. A LiF crystal was used to analyze chromium and iron, while nitrogen was measured by using synthetic LSM60 crystal. The setup procedure for quantitative analysis included the following steps: electron beam stabilization monitored by repetitive measurements of beam current in a Faraday cup and preliminary X-Ray acquisition from standards, which was used

to define the peak acquisition window and the background level for each element to be analyzed. Acquisition of X-Ray spectra of standard samples for chromium, iron and nitrogen. The set of standards included: an austenitic High Nitrogen Stainless Steel (18 wt-% Cr - 15 wt-% Mn - 0.39 wt-% N), solution treated at 1200°C during 6 hours and water quenched; high-purity CrN (50 at. %N) and Cr₂N (33.3 at. %N) nitrides in the form of thin layers (2.5-3 µm in depth) deposited onto carbon steel sheets by magnetron sputtering; conventional boron nitride pellets (50 at. %N), and high-purity electrolytic chromium flakes (99.99 wt. %Cr) and electrolytic nickel flakes (99.99 wt. %Ni). As a rule, in each experiment one of the chromium nitrides was chosen as standard and the other chromium nitride and the austenitic steel were supposed unknown. The acquisition of data from the steels only started when the measured nitrogen content of the “unknown” nitride was equal to the stoichiometric value and the measured nitrogen content of the austenitic HNSS was (0.39 ± 0.02) wt. %.

The representative size of the beam-specimen interaction volume was estimated by using the Kanaya-Okayama expression for the electron range [13], as follows:

$$d_{K-O} = \frac{0.000276A (E_0^{1.67} - E_c^{1.67})}{Z^{0.89} \rho} \quad (1)$$

where

E₀ = Energy of the incident beam in keV

E_c = Critical excitation energy in keV

ρ = Density in kg.m⁻³

Z = Atomic number.

Since the specimen is basically a Fe-22 wt. %Cr-5 wt. %Ni alloy, the value $Z = 0.73Z_{Fe} + 0.22Z_{Cr} + 0.05Z_{Ni} = 25.66$ was used.

Calculating d_{K-O} , for the analysis of nitrogen in the nitrided layer, we obtained $d_{K-O} = 1.52$ µm. The size of the beam-specimen interaction volume is of the order of magnitude of the thickness

of both layers, expanded ferrite and expanded austenite. Consequently, WDS technique was only used to measure the nitrogen content of the thick fully austenitic layer, obtained through HTGN.

X-Ray diffraction (XRD) was carried out in a Phillips diffractometer, using the θ - 2θ Bragg-Brentano configuration and Cu-K α radiation, $\lambda = 0.15418$ nm, with a scan rate of $0.02^\circ/\text{min}$, and 2θ varying from 20 to 120° . Picard's equation $a\gamma\text{N} = a\gamma + \kappa C_{\text{N}}$ was used to estimate the nitrogen content of high nitrogen austenite obtained after HTGN and expanded austenite obtained after LTPN, using the average of the lattice parameters. In Picard's equation, κ is equal to 0.00078 nm/at% N for concentrations up to 10 at% N. These calculations do not consider the effect of compressive residual stresses on the shift of diffraction peaks.

The crystal structures of the phases at the sample surface were also studied using an electron back scattering diffraction TSL-EBSD instrument, interfaced with a XL30 Philips scanning electron microscope. The diffraction patterns were collected in areas of 1.5×1.5 mm².

Specimens for transmission electron microscopy (TEM) analysis were prepared in a 3D FEG-FIB-SEM equipment to analyse the structure of the plasma nitrided layer formed on the single active screen plasma nitrided (ASPN) specimens. TEM analysis were carried out in a JEOL JEM-2100 transmission electron microscope.

Vickers microhardness tests were performed on a Shimadzu Microhardness HMV-2 tester using a Vickers indenter with a 0.1 N load, for measuring the hardness of the thin expanded ferrite and expanded austenite layers, formed after LTPN. These measurements were made on top of each expanded phase. Microhardness measurements for obtaining the hardness variation with depth below the nitrided surface, after HTGN, was carried out in the same HMV-2 tester, using a 1 N load. These measurements were taken on the transverse section of polished microstructure. ~~for measuring hardness of ferritic-austenitic matrix and the fully austenitic layer obtained after HTGN.~~

3 Results and Discussion

3.1 Microstructures and X-ray Characterization

As received

The microstructure of the as received UNS S31803 DSS is composed of austenite and ferrite stringers aligned in the rolling direction, as shown in Figure 1.

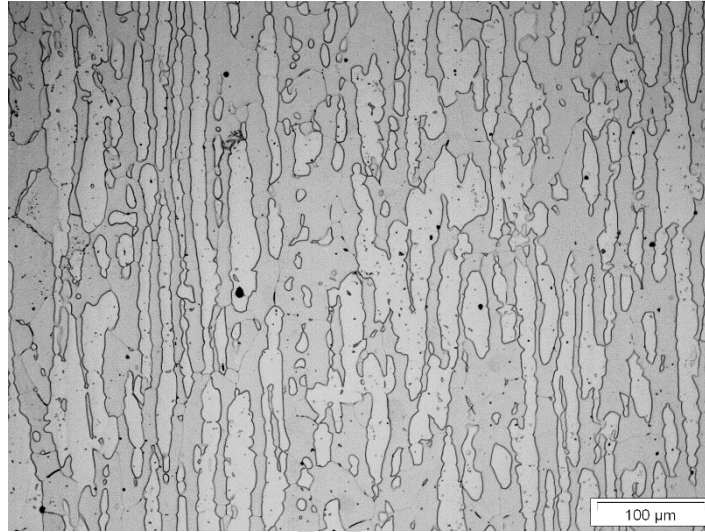


Figure 1. As received microstructure of the UNS S31803 steel. LOM.

Figure 2 shows the diffraction pattern of the as received UNSS31803 stainless steel. One can see ferrite and austenite peaks in the diffraction pattern of Figure 2, corresponding to ferrite and austenite stringers seen in Figure 1.

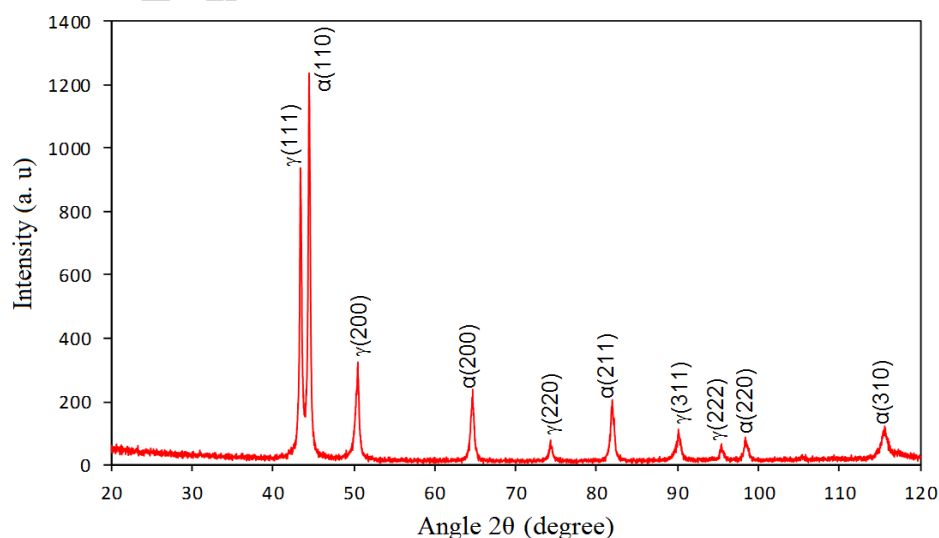


Figure 2 – Diffraction pattern of the as received UNS S31803 duplex stainless steel.

Single low temperature plasma nitriding

The LTPN single treated specimens showed diffraction patterns containing expanded austenite and expanded ferrite peaks as well as austenite and ferrite peaks from the bulk substrate, as shown in Figure 3.

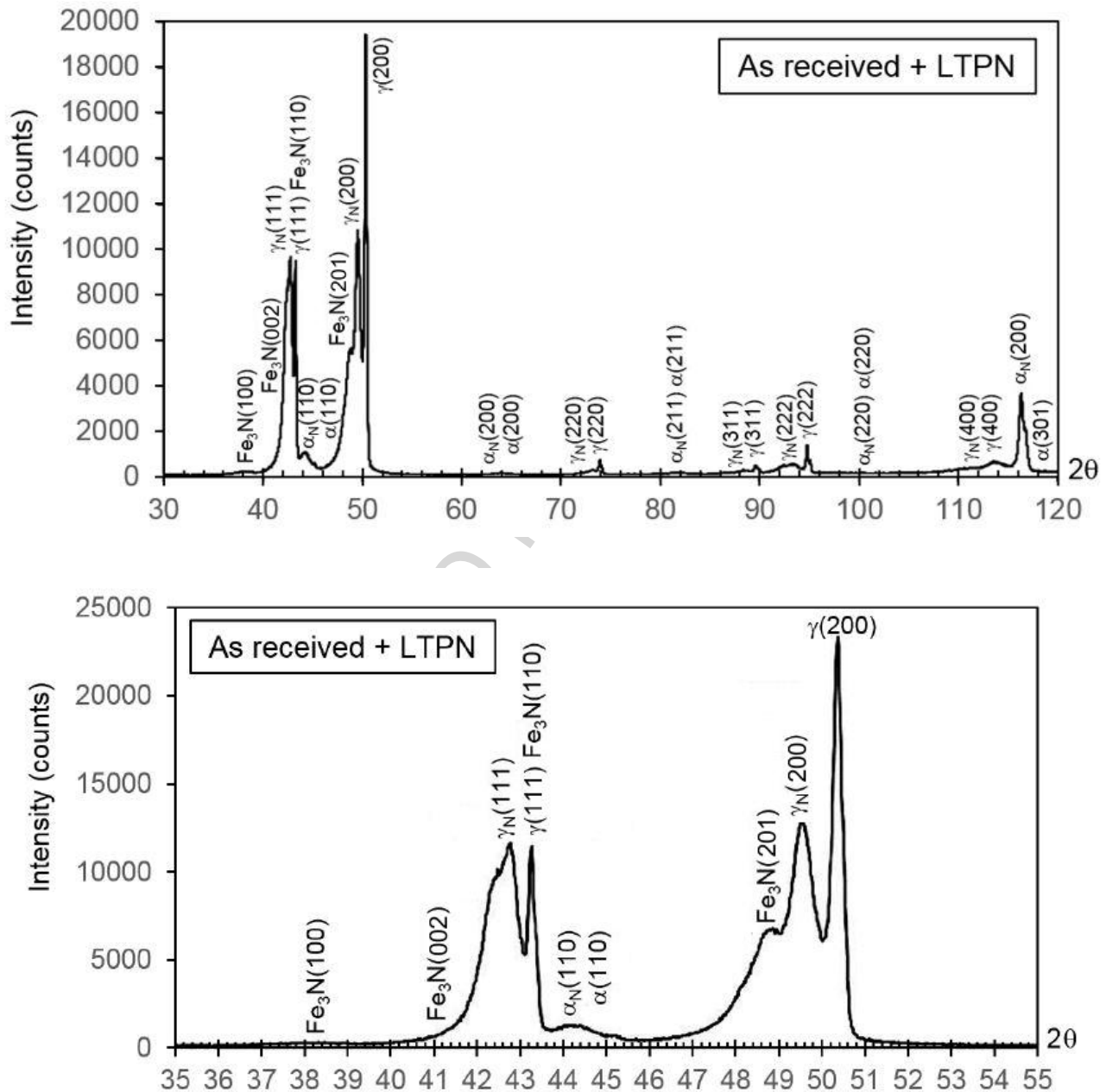


Figure 3. (a) XRD diffraction pattern of the single LTPN UNS S31803 steel; (b) detail of the XRD diffraction pattern ranging from 35° to 55° .

The expanded austenite peaks are shifted to lower diffraction angles; the calculated lattice parameter 0.36628 nm is higher than the austenite lattice parameter given in the reference card # 31-0619. ~~calculated for the as-received material 0.3613 nm. The calculated nitrogen content for γ_N (not considering the compressive residual stresses effects) is 13.7 at.% or 3.8 wt.%, very close to the reported 3.7 at.% N obtained by WDX for expanded austenite formed on a F51 duplex stainless steel [11].~~ This strong supersaturation and lattice expansion lead to strong hardening of the expanded austenite 1360 ± 81 HV 0.01. Expanded ferrite peaks can also be observed, shifted to lower diffraction angles compared to the BCC peaks of the substrate. The expanded ferrite peaks are broader than the substrate peaks, indicating the presence of compressive residual stresses due to nitrogen supersaturation. The average lattice parameter calculated for the α_N peaks is 0.2886 nm, higher than that found for the bulk ferrite peaks, 0.2867 nm. Nitrogen supersaturation causes a lattice expansion, increasing the hardness of expanded ferrite. Satyapal et al. [15] also reported a shift in peaks of austenite and ferrite due to the diffusion of nitrogen in the lattice of the substrate leading to an expansion of the lattice, and to the formation of expanded austenite and ferrite phases.

Not only γ , γ_N , α and α_N peaks were observed in the diffraction pattern in Figure 3, but also less intense ϵ -nitride (Fe_3N) peaks, indicating the presence of this phase, even though in small volume fractions. The precipitated nitrides could be contributing to the high hardness of the expanded ferrite regions, 1510 ± 52 HV 0.01. Sousa et al. [16] observed the formation of expanded ferrite after plasma nitriding of an AISI 409 ferritic stainless steel and reported the precipitation of ϵ -nitride (Fe_3N) in the expanded ferrite formed in the nitrided layer, as well.

The single LTPN treatment of UNS S31803 DSS resulted in a nitrided case composed by expanded austenite (γ_N) and expanded ferrite (α_N), formed on top of austenite and ferrite stringers, respectively. The expanded austenite regions of the nitrided case are thinner (~ 2.5 μm) than the expanded ferrite regions (~ 3.0 μm), probably due to the lower nitrogen diffusion coefficient in austenite compared to ferrite. Figure 4 shows the microstructure of the surface of the duplex UNS

S31803 steel after single LTPN. Inside the expanded ferrite regions, aligned bands can be seen indicating either intense deformation or precipitation of phases, not clearly identified through SEM examination [11].

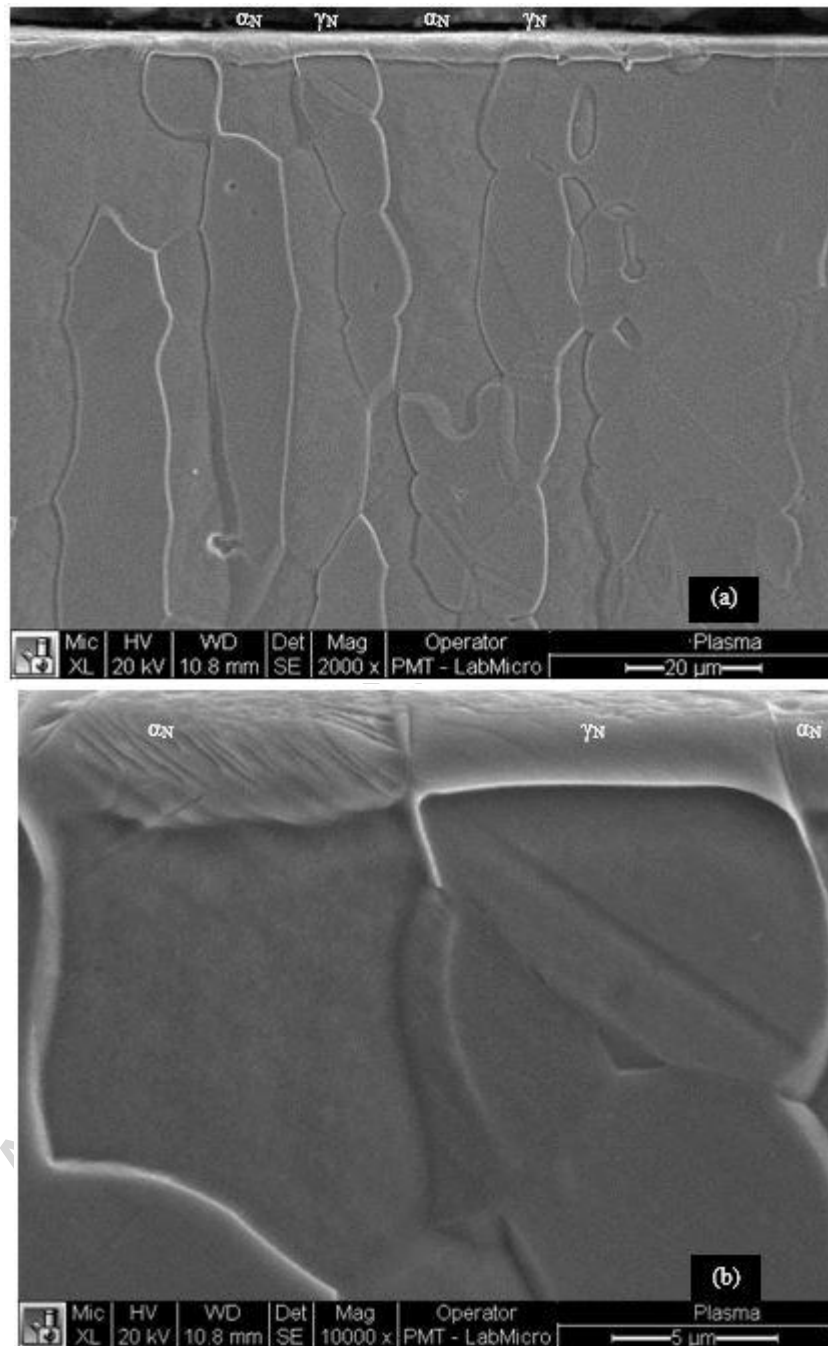


Figure 4. Microstructure of the UNS S31803 after LTPN. Expanded ferrite and expanded austenite in the nitrided layer.

EBSD analysis was carried out to better identify the expanded phases formed in the nitrided layer. Figure 5 (a) shows Phase ID mapping of the LTPN nitrided case (indicated by dashed white lines) and Figure 5 (b) the Confidence Index of the EBSD collected data. One can see that FCC expanded austenite (red) formed on FCC austenite grains (red) of the substrate and BCC expanded ferrite (predominantly green) formed on BCC ferrite grains (green) of the substrate. It is worth noting that the confidence index (CI) of the EBSD mapping is poor in the expanded ferrite regions, as shown in Figure 6 (b), probably due to precipitation of other phases in these regions.

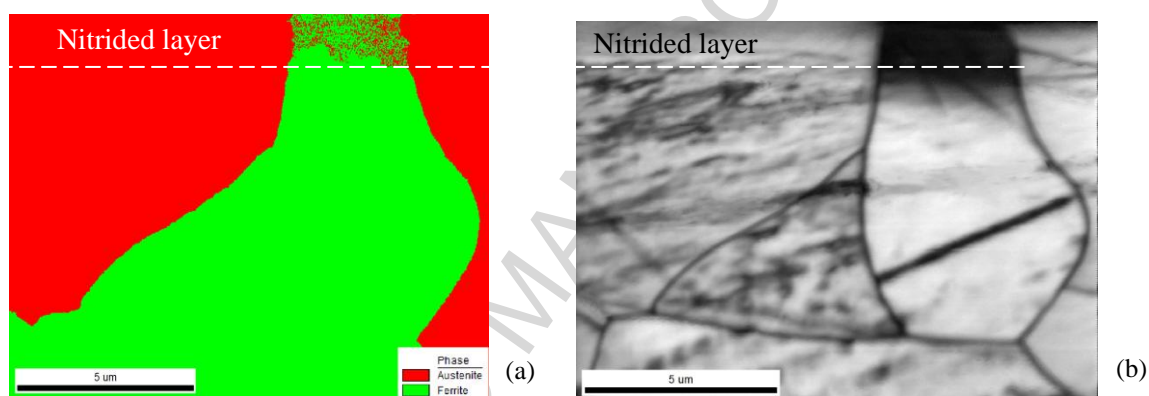


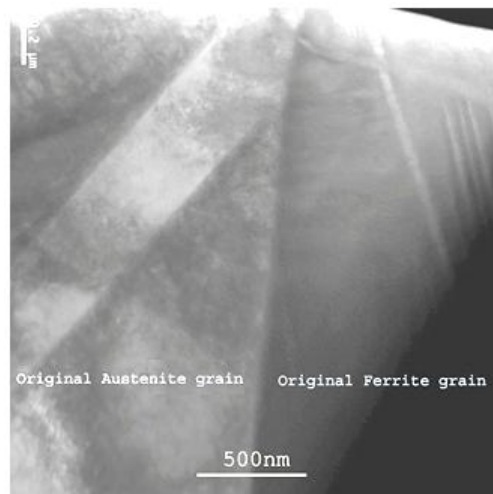
Figure 5. Phase ID (a) and Confidence Index CI (b) of the LTPN UNS S31803 steel. Red grains are FCC austenite and green grains are BCC ferrite. The dark region in (b) corresponds to a low Confidence Index (CI) region.

Although the character of the low Confidence Index, predominantly green region, could not be unambiguously defined, there are no signs of being composed by a fully expanded austenite region as reported in literature by Christiansen et al. [8] and Nagatsuka et al. [10]. Bielawski et al. [7] also reported low Confidence Indexes in similar regions in the nitrided layer of a duplex stainless steel, but did not identify them as expanded ferrite or expanded austenite.

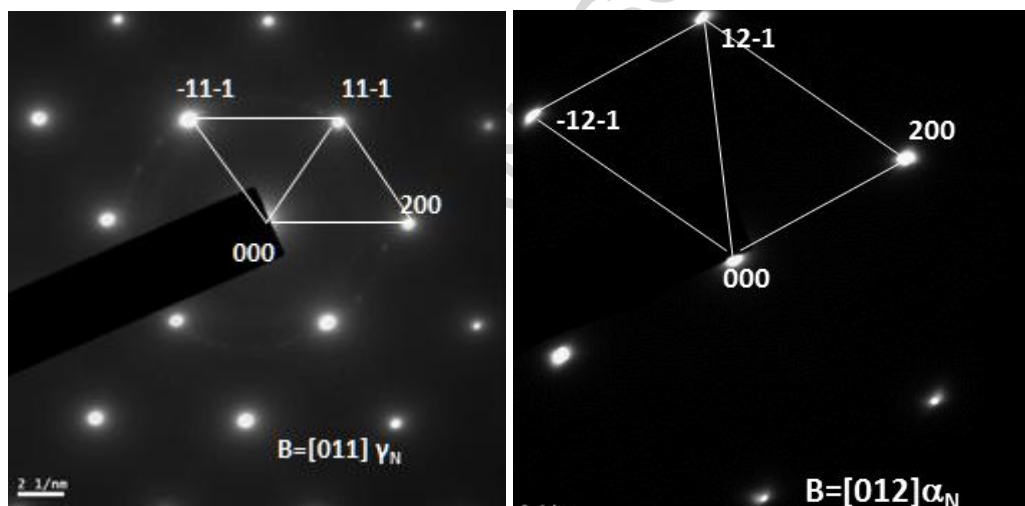
TEM analysis of the cross-section of the nitrided layer of the single plasma nitrided sample is shown in Figure 6 (a) and Figures 6 (b) and (c) are the corresponding SAD patterns to the left and right grains of Figure 6 (a). SAD patterns were firstly taken from the areas 5 μm below the surface

of the both grains to confirm the original structure of them. It was found that it was austenite and ferrite grains for the left and right grains, respectively.

Analysis of the SAD patterns taken from the left grain in Figure 6 (a) revealed an FCC structured pattern of zone B=[110]. When moving up the selected area from the area 5 μm below the surface, to the area close to the surface, the [110] SAD pattern and the orientation remained the same. D-spacing calculation from the SAD pattern from top and down areas revealed that the d-spacing of d111 is 0.212 nm and 0.208 nm respectively. This finding is similar to the results of low temperature plasma nitrided austenitic stainless steels [2]: nitrogen was introduced by plasma nitriding into the austenite interstitial places and formed a nitrogen supersaturated layer, or so-called S-phase layer. Figure 6 (c) is the SAD pattern taken from the matrix of the right grain in Figure 6 (a) and the indexing shows a [012] BCC pattern with the crystal constant of $a=0.2900$ nm, larger than the 0.2886 nm parameter estimated by XRD and larger than untreated ferrite ones ($a=0.2867$ nm). When moving the samples from the top to the down side of the ferrite grain (out of the nitride surface layer), the SAD patterns keep the same orientation but the deformed diffraction spots featured in Figure 6 (c) were getting sharp and normal. As can be seen in Figures 7 (a) and 8 (a), thin slabs were formed within ferrite grains. These slabs were identified as $\epsilon\text{-Fe}_3\text{N}$ nitride, precipitated from nitrogen-saturated ferrite (α_{N}) during plasma nitriding, as shown in Figure 7 (b). In Figure 7 (b), simulated and experimental SAD patterns of the $\epsilon\text{-Fe}_3\text{N}$ nitride and bcc ferrite phases indicate an orientation relationship of $[111]\alpha // [120]\epsilon\text{-Fe}_3\text{N}$, as can be seen by the double spots originated from the hexagonal and bcc phases.



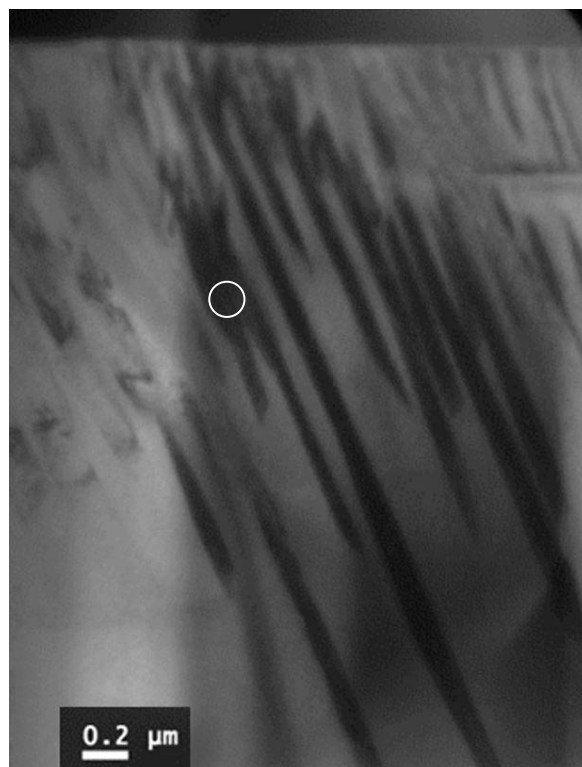
(a)



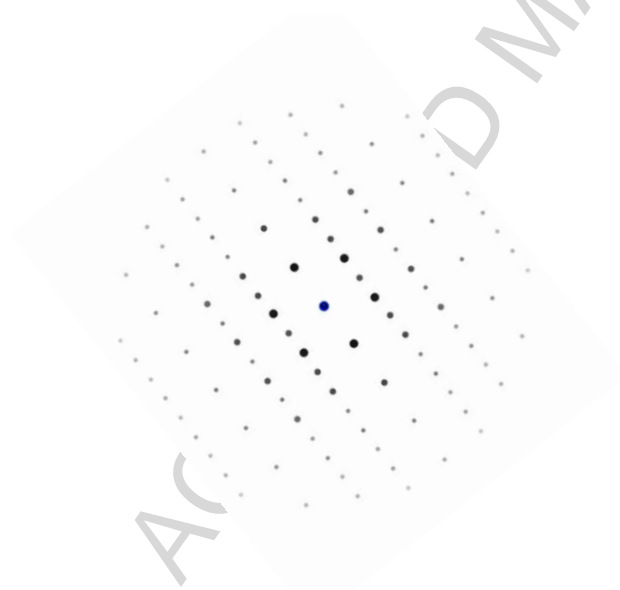
(b)

(c)

Figure 6 - TEM microstructure of a region with expanded austenite (left) and ferrite (right) (a) and the corresponding SAD patterns of a FCC - Zone axis $B = [011]\gamma_N$ (b) and BCC (c) phases - Zone axis $B = [012]\alpha_N$

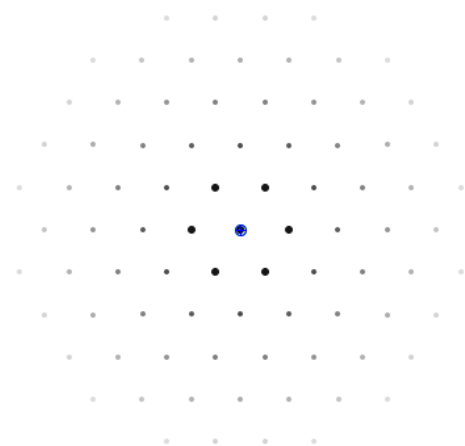


(a)



$(-1, 2, 0), LZ : 0$

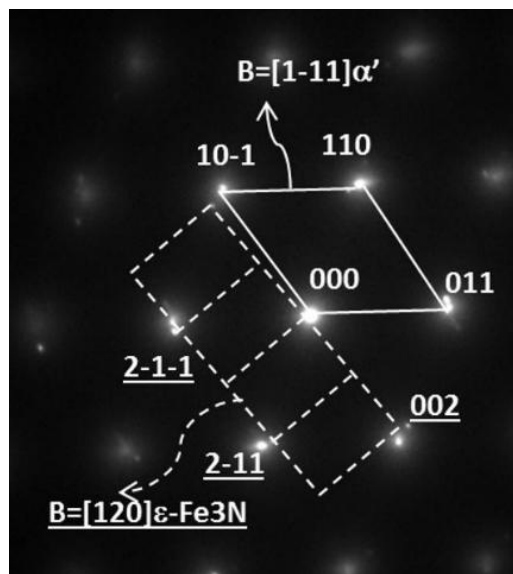
Center of Laue circle : (0.000, 0.000, 0.000)::Zone axis : [2, 1, 0]=[1, 0, -1, 0]
Tilt angle / deg. : 0.00



$(-1, 1, 0), LZ : 0$

Center of Laue circle : (0.000, 0.000, 0.000)::Zone axis : [1, 1, 1]
Tilt angle / deg. : 0.00

(b)



(c)

Figure 7 – (a) TEM microstructure; (b) simulated SAD patterns of expanded ferrite with ϵ -Fe₃N nitride precipitates and (c) experimental SAD patterns of expanded ferrite with ϵ -Fe₃N nitride precipitates. Zone axis $B = [120] \epsilon\text{-Fe}_3\text{N}$ and $B = [1-11] \alpha_N$.

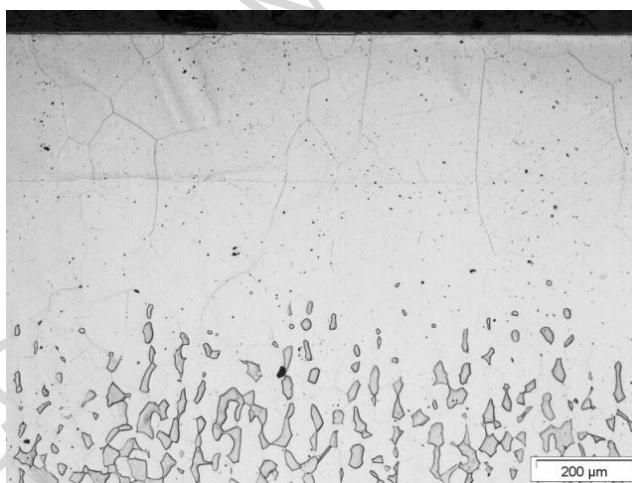
The above results suggest that the very high hardness obtained in the expanded ferrite regions of the nitrided layer, could be due to precipitation hardening of expanded ferrite by coherent ϵ -nitride precipitates. The ϵ -nitride precipitation could also be responsible for the observed low confidence index of the expanded ferrite regions of the single LTPN nitrided layer, shown in Figure 5. The obtained results herein differ from those obtained by Nagastuma et al. [10], which reports the formation of S phase on top of the entire microstructure of a superduplex stainless steel, after Active Screen Plasma Nitriding. However, the experimental conditions in both research works are very different (chemical composition of the steel, chemical composition of the active screen, chemical composition of the nitriding atmosphere, distance of the specimen to the active screen, etc.). Most probably, they had a great influence of the chemical composition of the species leaving the active screen towards the specimen, allowing the stabilization of S phase on top of ferrite grains.

Duplex nitriding treatment

The duplex surface treatment combining HTGN and LTPN changed completely the original microstructure of the UNS S31803 DSS, at the surface. Figure 8 (a) shows the microstructure of the UNS S31803 DSS after HTGN carried out at 1200 °C and 0.1 MPa for 8 hours and LTPN at 400 °C for 20 hours.

A fully austenitic layer, 550 μm in thick, is formed due to nitrogen pick-up and diffusion towards the center of the specimen, as a consequence of the exposure of the DSS to a high purity N_2 atmosphere during the HTGN treatment. Thermocalc® phase diagram, using TCFE database [17], predicts a 0.9 wt. % N fully austenitic microstructure in equilibrium with N_2 gas at 1200°C and 0.1 MPa, at the surface of the specimens, as shown in Figure 8(b). Nitrogen in solution destabilizes the ferrite stringers, transforming them into austenite. Consequently, intensive grain growth of austenite can be observed. WDS measurements of the nitrogen content on the surface of the nitrided layer, gave 0.89 ± 0.05 wt. % N, in accordance with the predicted value.

(a)



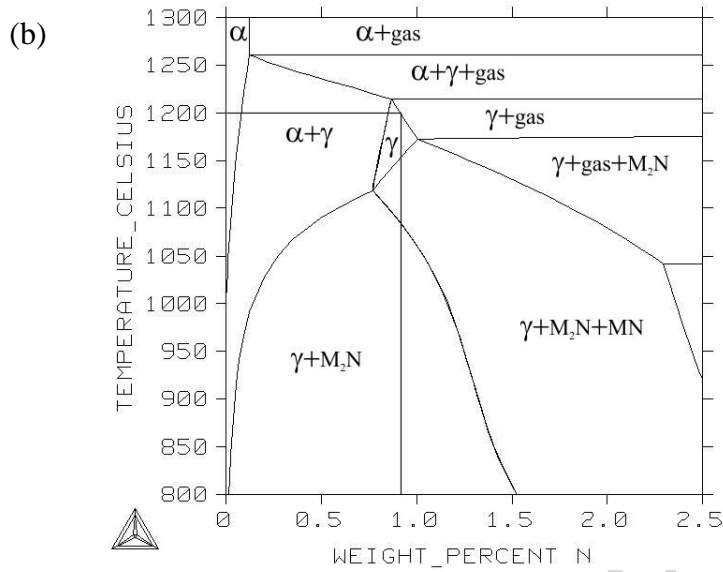


Figure 8. (a) Microstructure of the duplex (HTGN+LPTN) treated UNS S31803 DSS (LOM); b) isopleth of the UNS S31803 DSS in equilibrium with a 0.1 MPa N_2 pure atmosphere, as calculated by Thermocalc®, using TCFE database [17].

Figure 9 shows the N_2 solid solution hardening effect due to enrichment of the surface after HTGN. A layer of hardened austenite formed at the surface of the UNS 31803 DSS, providing a mechanical reinforcement of the soft matrix, increasing the load bearing capacity for the harder expanded austenite layer. Maximum hardness at the top of the 550 μm thick HTGN layer reached 329 ± 4 HV, decreasing to 280 HV, the base hardness of the UNS S 31803 DSS.

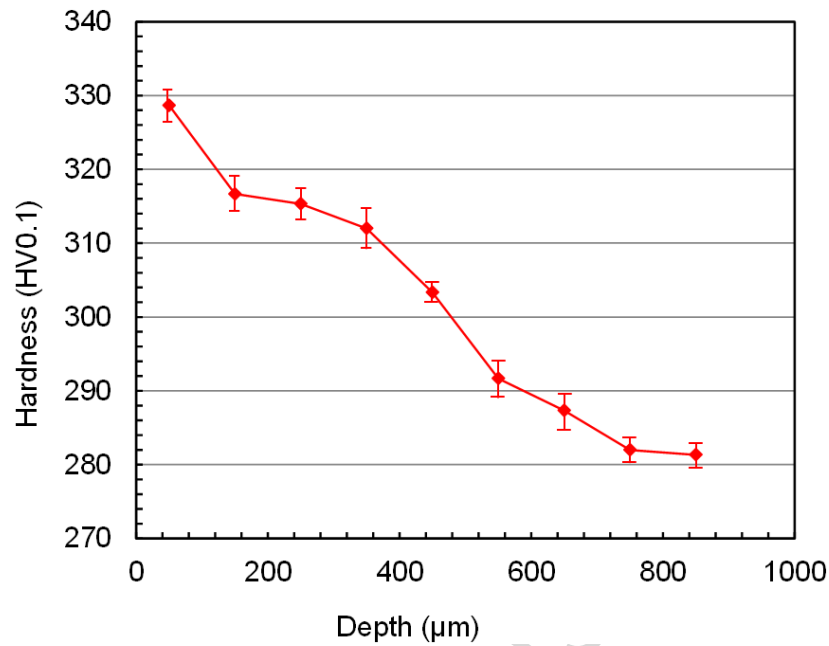


Figure 9. HV 0.1 microhardness across the austenitic case formed during HTGN.

The subsequent LTPN treatment enriched even more this austenite, fully transforming it into expanded austenite, as observed in Figure 10. The 4.3 μm thick expanded austenite layer is 1227 ± 78 HV0.01.

The duplex nitriding treatment resulted in a functionally graded material with a hardness variation from 1227 ± 78 HV to ≈ 330 HV and ≈ 280 HV.

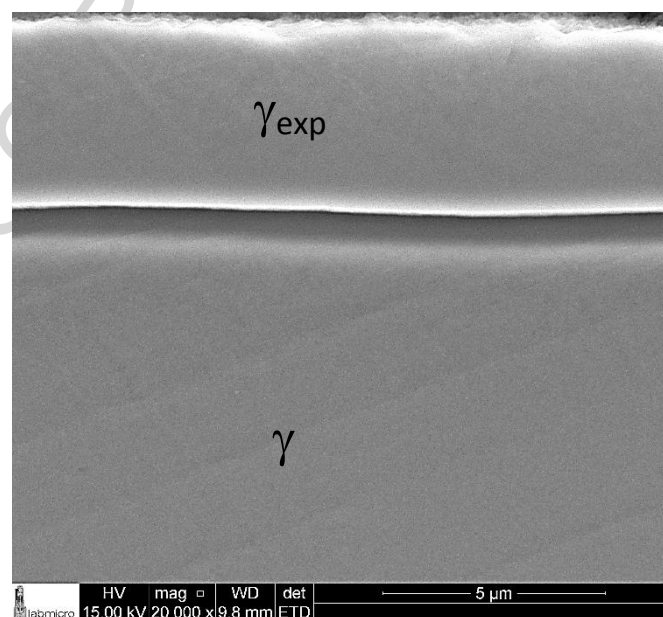


Figure 10. SEM image of the duplex HTGN+LTPN treated specimen.

X-ray diffraction

Figure 11 shows the XRD diffraction patterns of the simply HTGN UNS S31803 specimens. While the diffraction pattern of the as received samples (Figure 2) clearly show peaks corresponding solely to ferrite and austenite phases present in the bulk duplex microstructure, the diffraction pattern of the HTGN specimens exhibit only peaks of austenite. The austenite average lattice parameter, measured after HTGN is 0.3622 nm. Picard's equation ($a_{\gamma_N} = a_{\gamma} + 0.00078 C_N$) [18] using Vegard's constant 0.00078 nm/at% N, valid up to 10 at% N, allows calculating the nitrogen content (C_N) of the high nitrogen austenite (a_{γ_N}) obtaining a value of 0.92 wt.% nitrogen, in accordance to the Thermocalc® prediction presented in Figure 8(b) and also with the WDS measurements mentioned above.

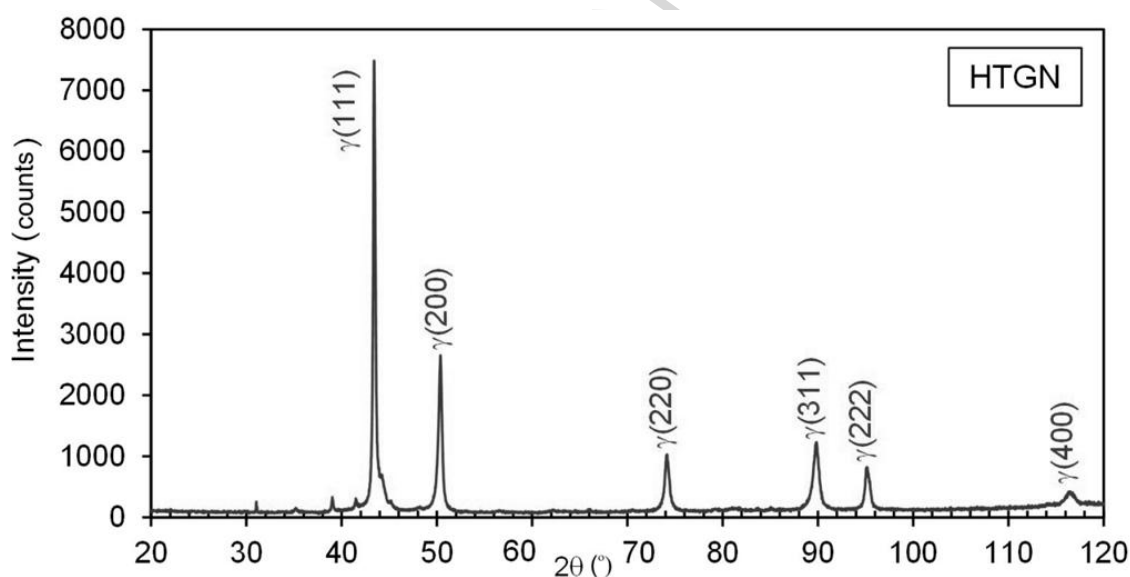
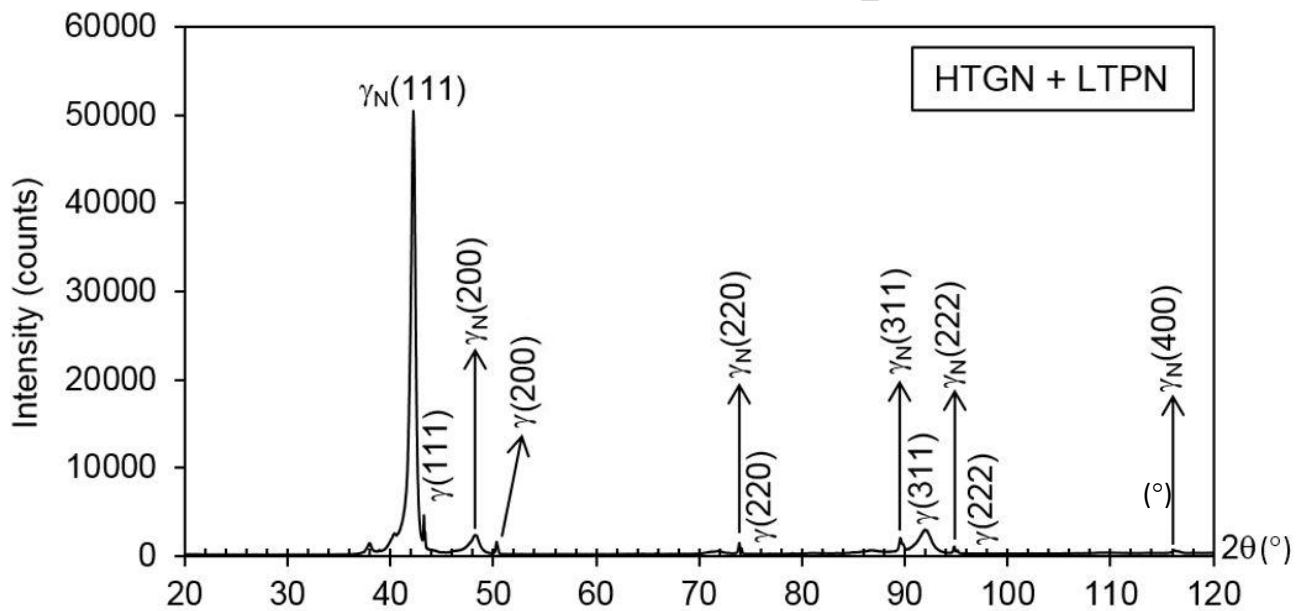


Figure 11. XRD diffraction pattern of the HTGN UNS S31803 stainless steel.

Figure 12a shows the XRD diffraction pattern for the duplex treated material (HTGN + LTPN). Pairs of FCC peaks are observed, corresponding to the $\gamma(111)$, $\gamma(200)$, $\gamma(220)$, etc. positions. Due to the low thickness of the LTPN layer, the incident X-ray beam is also diffracting in the fully non-expanded austenitic substrate. The peaks located in the right position correspond to the austenitic substrate reflections; while the peaks shifted to lower diffraction angles correspond to the γ_N expanded austenite phase. It is worth noting that the expanded austenite peaks are asymmetric, as

shown in the details (Figure 12b), indicating that nitrogen gradients are present in the expanded austenite phase. The calculated lattice parameter (not considering compressive residual stresses effects) for the γ_N expanded austenite phase is 0.3663 suggesting a concentration around 9.2 at.% N or 2.5 wt.% N. a value much lower than those reported for expanded austenite formed at the surface of austenitic AISI 316 stainless steel [2], partially explaining the lower γ_N expanded austenite hardness found in this work.



(a)

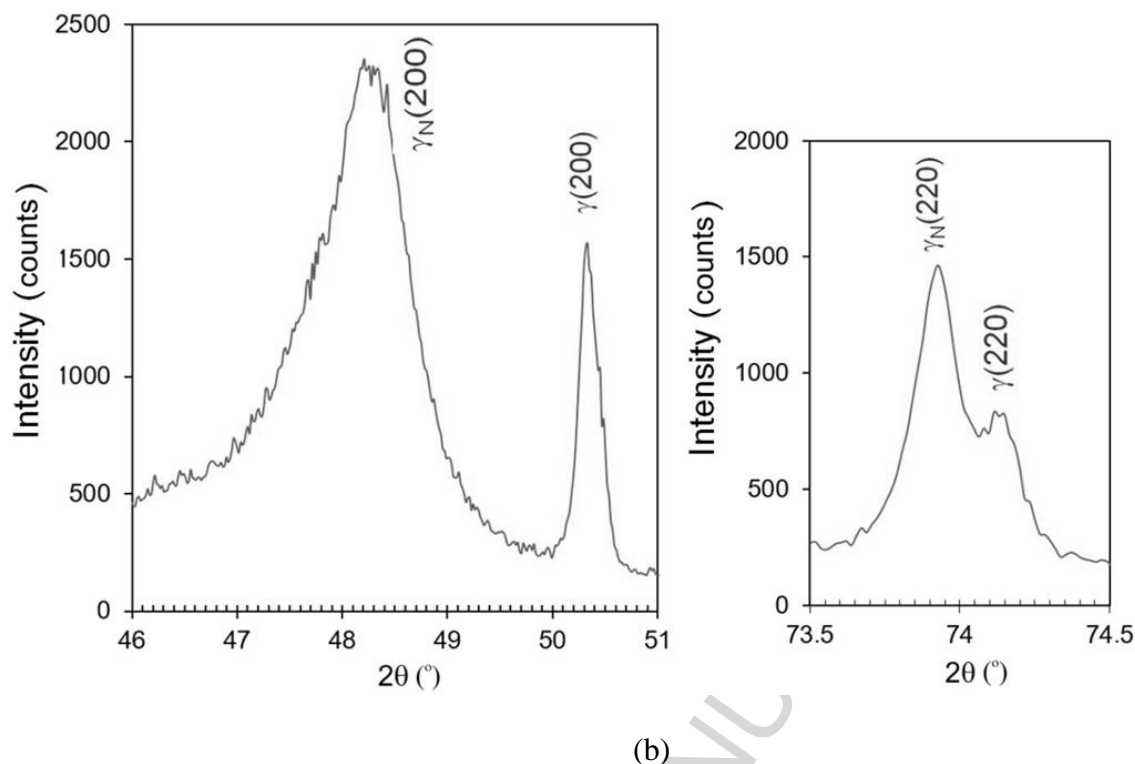


Figure 12. (a) XRD diffraction patterns for the duplex treated by high temperature gas nitriding and low temperature plasma nitriding (HTGN + LTPN) condition. (b) details of the XRD diffraction pattern for 2θ from 46° to 51° and from 73.5° to 74.5°.

Discussion

Duplex treatments usually combine thermochemical surface treatments such as nitriding or carburizing, with the subsequent deposition of a ceramic coating to obtain a surface with good tribological properties. A thick hardened layer grants mechanical support to a thinner ceramic coating deposited by some plasma-assisted process, PAPVD or PECVD [12]. Duplex thermochemical diffusion treatments consisting of two thermochemical diffusion treatments, one conducted at high temperature and a final one at low temperature (HTGN + LTPN) has never been discussed. Mesa et al. [13] proposed and carried out a duplex nitriding treatment for enhancing the cavitation erosion resistance of UNS S31803 duplex stainless steels, trying to improve the poor performance of LTPN duplex 2205 stainless steels, during cavitation erosion testing. The duplex

treated UNS S31803 stainless steel showed a more homogeneous variation of microstructure and less steep hardness gradients from surface towards the ferritic-austenitic core. Mesa et al. [13] studied methods for improving the cavitation erosion resistance of duplex UNS S31803 stainless steel. The idea was to compare the High Temperature Gas Nitriding with the Low Temperature Plasma Nitriding – LTPN surface treatments, carried out on a UNS S31803 duplex stainless steel. At first, a Low Temperature Plasma Nitriding – LTPN treatment was carried out on the UNS S31803 stainless steel, without success. The authors observed that the microstructure and mechanical properties of the LTPN nitrided layer was not homogeneous and did not perform very well under cavitation erosion conditions. Simultaneously, Mesa carried out a HTGN treatment on the UNS S31803 duplex stainless steel, obtaining much better cavitation-erosion results, indicating that the homogeneity of the surface microstructure (fully austenitic) and increased hardness (330 HV) could improve, significantly, the cavitation erosion-resistance of the UNS S31803 duplex stainless steel. Thereafter, the authors decided to investigate if a duplex nitriding treatment DN (HTGN + LTPN) could improve the performance of the duplex steel under cavitation erosion testing. The results indicated that the combination of the two thermochemical treatments resulted in a much better performance.

Comparison between the duplex treated UNS S31803 steel and a low temperature plasma nitrided UNS S30403 steel, resulted in incubation times almost 9 times greater. The maximum cavitation wear rate of the LTPN UNS S30403 was $5.5 \text{ g/m}^2\text{h}$, 180 times greater than the one measured for the duplex treated UNS S31803 steel. The greater cavitation wear resistance of the duplex treated UNS S31803 steel, compared to the LTPN treated UNS S30403 steel was explained by the greater mechanical support the fully austenitic, 330 HV 0.1 hard, $100 \mu\text{m}$ layer gives to the expanded austenite layer formed on top of the specimen after LTPN. It was concluded that the greater mechanical support the thick HTGN nitride layer gives to the hard LTPN expanded austenite layer formed on top of the specimen, granted good adhesion of the expanded austenite

layer to the substrate increasing the incubation time for cavitation damage and decreasing the rate of mass loss during cavitation-erosion.

Indeed, the results reported hereby show that LTPN of the UNS S31803 duplex stainless steel promotes the formation of a duplex modulated structure composed by expanded ferrite and expanded austenite on ferrite and austenite grains, respectively. Although chromium nitrides could not be detected in the nitrided layer, intense coherent ϵ -Fe₃N nitride precipitation in the expanded ferrite phase was detected, which led to a strong increase in microhardness of the expanded ferrite regions. Very steep hardness gradients allows easy spalling and detachment of the thin and hard (expanded ferrite + expanded austenite) layer.

Pinedo et al. [11] reported a study, aiming a more fundamental understanding of what where the mechanisms involved in the LTPN surface treatment of duplex stainless steels. In their research work, carried out in a pulsed plasma DC reactor, the authors reported the formation of a modulated nitrided layer, composed of expanded ferrite on top of ferrite grains and expanded austenite on top of austenite grains of the duplex stainless steel microstructure, without any precipitation of chromium or iron nitrides. Some “deformation bands” were observed, inside expanded ferrite, which were assigned to intense compressive residual stresses. On the other hand, the results reported in this manuscript are quite different from those given in reference [11]. Although the modulated structure reported in the previous paper was also formed after active screen LTPN, the results show that ϵ -Fe₃N needles precipitate coherently inside the expanded ferrite regions of the nitrided layer, sharply increasing the hardness.

The duplex HTGN + LTPN nitriding treatment, consisting of a $\approx 4 \mu\text{m}$ thick, nitrogen rich, 1227 ± 78 HV 0.01 hard, expanded austenite layer, formed on top of a 550 μm thick, 0.9 wt% N, fully austenitic layer, ensures a more homogeneous microstructure and gentler hardness gradients. Accordingly, a better performance should be expected in wear bearing applications in which very

high loads and high stress concentration are applied, due to the increased load bearing capacity conferred by the High Temperature Gas Nitriding treatment.

4. Conclusions

- 1) The single 400°C low temperature nitriding treatment of the as received UNS S31803 duplex stainless steel led to formation of a modulated nitrated layer composed of expanded ferrite and expanded austenite, with hardness of 1510 ± 52 HV0.01 and 1360 ± 81 HV0.01, respectively. The expanded austenite formed on the austenite stringers of the microstructure, while the expanded ferrite formed on the ferrite stringers of the bulk microstructure.
- 2) Coherent ϵ -Fe₃N nitrides precipitated inside expanded ferrite with a $[111] \alpha // [120] \epsilon$ -Fe₃N orientation relationship.
- 3) High temperature gas nitriding of UNS S31803 stainless steel carried out at 1200°C, under 0.1 MPa and for 8 hours led to the formation of a 550 μ m thick high nitrogen fully austenitic layer at the surface of the specimens and to surface hardening of the DSS, up to 330 HV0.1.
- 4) The Duplex Treatment (High Temperature Gas Nitriding, carried out at 1200°C, 0.1 MPa for 8 hours, followed by Low Temperature Plasma Nitriding at 400°C, 75%N₂+25%H₂, 400 Pa pressure and 20 hours) resulted in a 1227 ± 78 HV hard, 4.3 μ m thick, expanded austenite layer, formed on top of a 330 HV hard, high nitrogen, fully austenitic layer.
- 5) ~~The duplex treatment may result in better wear performance of parts subjected to high levels of stress concentration~~

Acknowledgements

To the São Paulo State Research Foundation, FAPESP, process 2012/50890-0 and to the University of Birmingham, UK, for the financial support,.

References

- [1] I. Alvarez-Armas, Duplex Stainless Steels: Brief History and Some Recent Alloys, Recent Patents on Mechanical Engineering, 7 (2010) 51-57.
- [2] N. Mingolo, C.E. Pinedo, A.P. Tschiptschin - On the formation of expanded austenite during plasma nitriding of an AISI 316L austenitic stainless steel, Surface and Coatings Technology, 201 (2006) 4215-4218.
- [3] Y. Sun, T. Bell, G. Wood, Wear behavior of plasma-nitrided martensitic stainless steel, Wear 178 (1994) 131–138.
- [4] B. Larisch, U. Brusky, H.-J. Spies, Plasma nitriding of stainless steels at low temperatures, Surface and Coatings Technology 116–119 (1999) 205–211.
- [5] C. Blawert, B.L. Mordike, Y. Jiráskova, O. Schneeweiss, Structure and composition of expanded austenite produced by nitrogen plasma immersion ion implantation of stainless steels X6CrNiTi1810 and X2CrNiMoN2253, Surf. Coat. Tech. 116-119 (1999) 189-198.
- [6] J. Bielawski, J. Baranowska, Microstructure and properties of layers on chromium steel, Surf. Coat. Tech., 200 (2006) 6572-6577.
- [7] J. Bielawski, J. Baranowska, Formation of nitrided layers on duplex steel – influence of multiphase substrate, Surf. Eng. 26 (2010) 299-304.
- [8] T. Christiansen, M.A.J. Somers, Characterisation of low temperature surface hardened stainless steel, E-Structure, Struers Journ. of Materialog. 9 (2006) 1-17.
- [9] L. H. Chiu , Y. Y. Su , F. S. Chen, H. Chang - Microstructure and Properties of Active Screen Plasma Nitrided Duplex Stainless Steel, Journal Materials and Manufacturing Processes, 25 (2010) 316-323.
- [10] K. Nagatsuka, A. Nishimoto, K. Akamatsu - Surface hardening of duplex stainless steel by low temperature active screen plasma nitriding, Surface and Coatings Technology, 205 (2010) S295-S299.

- [11] C.E. Pinedo, L.B. Varela, A.P. Tschiptschin, Low-temperature plasma nitriding of AISI F51 duplex stainless steel, *Surface & Coatings Technology*, 232 (2013) 839–843.
- [12] Tschiptschin, A.P. Duplex Coatings. In: Wang, Q. Jane; Chung, Yip-Wah. (Org.). *Encyclopedia of Tribology*. 1ed. Munich: Springer US, 2013, v. 2, p. 794-800.
- [13] D.H. Mesa, C.E. Pinedo, A.P. Tschiptschin, Improvement of the cavitation erosion resistance of UNS S31803 stainless steel by duplex treatment, *Surface & Coatings Technology* 205 (2010) 1552–1556.
- [14] A. Toro; A. P. Tschiptschin - Chemical characterization of a high nitrogen stainless steel by optimized electron probe microanalysis - *Scripta Materialia* 63 (2010) 803-806.
- [15] M. Satyapal, A.S. Khanna, A. Joseph - Effect of Temperature on the Plasma Nitriding of Duplex Stainless Steels – *International Journal of Engineering and Inonovative Technology* – 2 (2013) 217-222.
- [16] R.R.M. Sousa, F.O. Araújo, J.A.P. Costa, A.A. Oliveira, M.S. Melo, C.A. Alves Jr. Cathodic Cage Nitriding of AISI 409 Ferritic Stainless Steel with the Addition of CH₄ *Materials Research* 15 (2012) 260-265.
- [17] Thermo-Calc Software – TCF8 – TCS Steels/Fe-Alloys Database, Version 8.0 – http://www.thermocalc.com/media/31186/Upgrade_TCFE8-from-TCFE7.pdf . Acessed june 20, 2017.
- [18] S. Picard, J.B. Memet, R. SABOT, J.L. Grosseau-Poussard, J.P. Rivière, R. Meilland, Corrosion behavior, microhardness and surface characterization of low energy, high current ion implanted austenitic stainless steel. *Materials Science and Engineering A*, 303 (2001) 163-172.

Figure captions:

Figure 1. As received microstructure of the UNS S31803 steel. LOM.

Figure 2 – Diffraction pattern of the as received UNS S31803 duplex stainless steel.

Figure 3. (a) XRD diffraction pattern of the single LTPN UNS S31803 steel; (b) detail of the XRD diffraction pattern ranging from 35° to 55°.

Figure 4. Microstructure of the UNS S31803 after LTPN. Expanded ferrite and expanded austenite in the nitrided layer.

Figure 5. Phase ID (a) and Confidence Index CI (b) of the LTPN UNS S31803 steel. Red grains are FCC austenite and green grains are BCC ferrite. The dark region in (b) corresponds to a low Confidence Index (CI) region.

Figure 6 - TEM microstructure of a region with expanded austenite (left) and ferrite (right) (a) and the corresponding SAD patterns of a FCC (b) and BCC (c) phases.

Figure 7 – (a) TEM microstructure; (b) simulated SAD patterns of expanded ferrite with ϵ -Fe₃N nitride precipitates and (c) experimental SAD patterns of expanded ferrite with ϵ -Fe₃N nitride precipitates.

Figure 8. (a) Microstructure of the duplex (HTGN+LTPN) treated UNS S31803 DSS (LOM); b) isopleth of the UNS S31803 DSS in equilibrium with a 0.1 MPa N₂ pure atmosphere, as calculated by Thermocalc®, using TCFE database.

Figure 9. HV0.1 microhardness across the austenitic case formed during HTGN.

Figure 10. SEM image of the duplex HTGN+LTPN treated specimen.

Figure 11. XRD diffraction pattern of the HTGN UNS S31803 stainless steel.

Figure 12. (a) XRD diffraction patterns for the duplex treated by high temperature gas nitriding and low temperature plasma nitriding (HTGN + LTPN) condition. (b) details of the XRD diffraction pattern for 2 θ from 46° to 51° and from 73.5° to 74.5°.

Highlights

- LTPN of 31803 DSS forms a nitrided layer composed by expanded γ_N and α_N phases.
- During LTPN, ϵ -Fe₃N nitrides precipitate in α_N with $[120]\epsilon\text{-Fe}_3\text{N}/[111]\alpha_N$.
- A duplex nitriding (DN) treatment (HTGN+LTPN) of 31803 DSS was developed.
- (DN) formed a $\sim 4\text{ }\mu\text{m}$ thick expanded γ_N layer on top of a $550\text{ }\mu\text{m}$ thick γ layer.
- (DN) case microstructure is fully austenitic showing gentler hardness gradients.